Characterization of the Efflux Transporter(s) Responsible for Restricting Intestinal Mucosa Permeation of an Acyloxyalkoxy-Based Cyclic Prodrug of the Opioid Peptide DADLE

Fuxing Tang[1,2] and Ronald T. Borchardt[1,2,3]

Received February 19, 2002; accepted February 28, 2002

Purpose. To elucidate the efflux transporter(s) responsible for restricting the permeation of an acyloxyalkoxy-based cyclic prodrug of the opioid peptide DADLE (AD) through Caco-2 cell monolayers.
Methods. The cellular permeation characteristics of AD were investigated using Caco-2 cells, Madin–Darby canine kidney wild-type II cells (MDCK-WT), MDCK cells transfected with the human MDR1 gene (MDCK-MDR1), and MDCK cells transfected with the human MRP2 gene (MDCK-MRP2). These cells were grown as monolayers onto microporous membranes. The disappearance of AD from the donor side and its appearance on the receiver side were monitored by high-performance liquid chromatography. The substrate activity of AD for P-glycoprotein (P-gp) was determined using GF120918, a known P-gp specific inhibitor. The substrate activity of AD for MRP2 was determined by using cyclosporin A, a known MRP2 and P-gp inhibitor.
Results. In Caco-2 cells, the ratio of the apparent permeability coefficients (P_{app}) of AD flux measured in the basolateral (BL) to apical (AP) direction vs. the flux in the AP-to-BL direction ($P_{app\ BL\text{-}to\text{-}AP}/P_{app\ AP\text{-}to\text{-}BL}$) was 99. In the presence of 2 μM GF120918 or 25 μM cyclosporin A, the $P_{app\ BL\text{-}to\text{-}AP}/P_{app\ AP\text{-}to\text{-}BL}$ ratio was decreased to 11. In MDCK-WT, MDCK-MDR1, and MDCK-MRP2 cells, the $P_{app\ BL\text{-}to\text{-}AP}/P_{app\ AP\text{-}to\text{-}BL}$ ratios of AD were 4.7, 10, and 5.8, respectively. A mixture of GF120918 (2 μM) and cyclosporin A (25 μM) decreased the $P_{app\ BL\text{-}to\text{-}AP}/P_{app\ AP\text{-}to\text{-}BL}$ ratios of AD in MDCK-WT, MDCK-MDR1, and MDCK-MRP2 cells to 1.2, 1.8, and 2.3, respectively.
Conclusions. These data suggest that AD is a much better substrate for P-gp than MRP2 and that the restricted permeation of this cyclic prodrug in Caco-2 cells and in the intestinal mucosa probably is due primarily to its substrate activity for P-gp.

KEY WORDS: Caco-2 cell monolayer; DADLE; MDR 1; MRP 2; acyolxyalkoxy-based cyclic prodrug.

INTRODUCTION

Peptides, including opioid peptides, represent an important new class of potential drug candidates (1,2). However, the major obstacles impeding the clinical development of peptide-based drugs are their metabolic lability (hydrolytic) and their inability to permeate biologic barriers [e.g., intestinal mucosa, blood–brain barrier (BBB)] (3). The problem of metabolic lability (hydrolytic) has been resolved by medicinal chemists through the structural manipulation of the peptide bonds and the creation of peptidomimetics (4). However, this chemical strategy has not always led to peptide-based drug candidates with improved oral bioavailability and improved brain permeation (5,6). Peptidomimetics often exhibit low intrinsic permeability and/or substrate activity for efflux transporters that limit their intestinal permeation (7) and/or BBB permeation (8). In addition, these more lipophilic peptidomimetics often exhibit substrate activity for cytochrome P450 3A4, which can limit their oral bioavailability (9).

In recent years, our laboratory has described a cyclic prodrug strategy to improve the permeation of hydrophilic peptides through the intestinal mucosa and the BBB (10–12). Cyclic prodrugs prepared with a linker between the N-and C-terminal ends of peptides were shown to exhibit greater stability against exopeptidases (10,11). In addition, cyclization using these linkers was shown to restrict the conformational flexibility of the molecule and result in a more compact structure with more favorable physicochemical properties (e.g., β-turns) for cell permeation (13). More recently, our laboratory applied this cyclic prodrug strategy to synthesize an acyloxyalkoxy-based cyclic prodrug of the opioid peptide DADLE (H-Tyr-D-Ala-Gly-Phe-D-Leu-OH; AD; Fig. 1), which had improved metabolic stability to protease (14,15). A fundamental requirement for a successful peptide prodrug is the complete conversion of the prodrug to the peptide via chemical and/or enzymatic reactions. Indeed, AD was found to undergo bioconversion to DADLE in biologic media containing esterase activity (15). As expected, AD showed improved physicochemical properties (e.g., high lipophilicity and low hydrogen potential) as compared to DADLE, for cell permeation (14,15). However, when the cell permeation characteristics of AD were determined using Caco-2 cells, an *in vitro* model of the intestinal mucosa (16–18), it was found to be less permeable than DADLE when measured in the apical (AP) to basolateral (BL) direction (15). This very low permeation of AD was shown to result from its substrate activity for efflux transporters in Caco-2 cells (15). In recent years, the intestinal mucosa (19) and Caco-2 cells (20) have been shown to express efflux transporters [e.g., multidrug resistance (MDR) transporter (P-glycoprotein, P-gp) and multidrug resistance associated protein (e.g., MRP2)], which restrict the permeation of lipophilic drugs/drug candidates.

To elucidate which transporter(s) is/are responsible for restricting the permeation of AD through the Caco-2 cell monolayers, we used in this study Madin–Darby canine kidney (MDCK) cells transfected with human *MDR1* gene (MDCK-MDR1) and MDCK cells transfected with human *MRP2* gene (MDCK-MRP2). MDCK-MDR1 cells and MDCK-MRP2 cells overexpress human P-gp and MRP2 (21), respectively. Similar to the MDR1 and MRP2 expressed in Caco-2 cells, the human P-gp and MRP2 expressed in MDCK-MDR1 and MDCK-MRP2 cells are localized on the AP side of polarized cell monolayers, and these transporters efflux substrate drugs to the AP side of cell monolayers (21). Therefore, these cell lines can be used to elucidate the efflux transporter(s) responsible for restricting the cell permeation of AD.

[1] Department of Pharmaceutical Chemistry, The University of Kansas, Lawrence, Kansas 66047.
[2] Current address: Forest Laboratories, Inc., Farmingdale, New York 11735
[3] To whom correspondence should be addressed. (e-mail: rborchardt@ku.edu)

0724-8741/02/0600-0780/0 © 2002 Plenum Publishing Corporation

MATERIALS AND METHODS

Materials

AD was synthesized using the methods previously described by our laboratory (14). Caco-2 cells were obtained from the American Type Culture Collection (ATCC; Rockville, Maryland). MDCK strain II (MDCK-WT), MDCK-MDR1, and MDCK-MRP2 cells were gifts from Professor Piet Borst (The Netherlands Cancer Institute, Amsterdam, The Netherlands). GF120918 was donated by Dr. Kenneth Brouwer (GlaxoSmithKline, Research Triangle Park, North Carolina). Dulbecco's phosphate-buffered saline, Hanks' balanced salts (HBSS) (modified), cyclosporin A (CsA), acetonitrile, phosphoric acid, and trifluoroacetic acid were purchased from Sigma Chemical Co. (St. Louis, Missouri). L-Glutamine (200 mM), penicillin (10, 000 U/mL), streptomycin (10,000 μg/mL), and non-essential amino acids [10 mM (100×) in 85% saline] were obtained from Gibco BRL, Life Technologies (Grand Island, New York). Dulbecco's Modified Eagle Medium (DMEM) and trypsin/EDTA solution (0.25% and 0.02% respectively, in Ca^{+2} and Mg^{+2} free HBSS) were obtained from JRH Bioscience (Lenexa, Kansas). Rat-tail collagen (type I) was obtained from Collaborative Biomedical Products (Bedford, Massachusetts). Fetal bovine serum was obtained from Atlanta Biologicals (Norcross, Georgia). Polycarbonate Transwells® (3 μm pore size) and polyester Transwells® (0.4-μm pore size) were obtained from Corning Costar (Cambridge, Massachusetts). [^{14}C]-Mannitol (specific activity 51 mCi/mmol) and [^{3}H]-digoxin (specific activity 19 Ci/mmol) were purchased from NEN Life Science Products, Inc. (Boston, Massachusetts). The primary antibody mdr Ab-1 was purchased from Oncogene Science Corporation (Cambridge, Massachusetts). C219 was obtained from Signet Pathology Systems, Inc. (Dedham, Massachusetts). Anti-human MRP2 M_2I-4 was purchased from Kamiya Biomedical Company (Seattle, Washington).

Cell Culture

Caco-2 cells were seeded at 79,000 cells/cm^2 on Transwell® filter inserts (6 well) and maintained in high-glucose DMEM supplemented with 10% fetal bovine serum, 0.1 mM non-essential amino acids, 2 mM L-glutamine solution, 100 U/mL penicillin and 100 μg/mL streptomycin as described previously (22). Cells (passages 20–40) were used on days 21–28 post-seeding.

MDCK-WT, MDCK-MDR1, and MDCK-MRP2 cells were seeded at 50,000 cells/ cm^2 on polyester Transwell® filter inserts (6 well) and maintained under the same conditions as described above for Caco-2 cells. Experiments were conducted on these cells after 6 days of culture. The expression of P-gps and MRP2s in the transfected MDCK cells was confirmed by Western blotting and measuring the efflux of known substrates of these transporters (23,24). Briefly, proteins (10 μg for P-gp, 20 μg for MRP2) in the total cell lysates from Caco-2, MDCK-WT, MDCK-MDR1, or MDCK-MRP2 cell monolayers were size fractionated in 6% Tris-glycine polyacrylamide gel in 0.1% of SDS Tris-glycine buffer. After electroblotting, P-gps were stained with mdr Ab-1 and MRP2s were stained with M_2I-4. The protein-antibody interaction was visualized using the chemiluminescence technique. The cells were split twice a week with 1:10 dilution and used within 2 months after being removed from liquid N_2.

All cell lines were maintained at 37°C in a humidified 5% CO_2, 95% air atmosphere. The membrane integrity was checked using [^{14}C]-mannitol. The apparent permeability coefficients (P_{app}) of [^{14}C]-mannitol across Caco-2 and MDCK cell monolayers were typically in the range of 0.1–0.6 × 10^{-6} cm/s.

Transport Experiments

Bidirectional transport experiments were performed as previously described (22) with some modifications. All experiments were done at 37°C in air with constant mixing in a shaking water bath (60 rpm). Briefly, the AP and the BL chambers of each insert were washed twice with 37°C-HBSS for 15 m. Test drugs AD (75 μM), [^{3}H]-digoxin (0.011 μM), [^{3}H]-vinblastine (0.011 μM), or [^{14}C]-mannitol (0.011 μM) were added to the donor side (1.5 mL for AP chamber and 2.5 mL for BL chamber) and fresh HBSS was placed in the receiver compartment. To inhibit the activity of efflux transporters, cell monolayers were incubated with HBSS containing GF120918 (2 μM), CsA (25 μM), or a cocktail of GF120918 (2 μM) and CsA (25 μM) for an additional 15 min. The test compounds were then added to the donor side along with GF120918 (2 μM) and/or CsA (25 μM), and fresh HBSS containing inhibitor [i.e., GF120918 (2 μM) and/or CsA (25 μM)] was placed in the receiver side. Aliquots (100 μl) were withdrawn from the receiver side at various time intervals up to 80 min. Fresh HBSS or HBSS containing inhibitor (100 μL) was replaced in the receiver side after sampling. When radioactive substrates were used, radioactivity in aliquots from the donor and receiver sides of the monolayers was measured in a scintillation counter LS6001C (Beckman Instruments, Inc., Fullerton, California). In experiments using AD, aliquots were stabilized by the addition of aliquots of acetonitrile [10% (v/v)] and diluted phosphoric acid [0.1% (v/v)]. The acidic mixture was immediately analyzed at 4°C using high-performance liquid chromatography (HPLC) or frozen and kept at −80°C until HPLC analysis.

[^{3}H]-Digoxin, a substrate for P-gp (23), and [^{3}H]-vinblastine, a substrate for both P-gp and MRP2 (24) were used to check the functional efflux activity of P-gp and MRP2 in these cell models (23–24). The ratios of $P_{app\ BL\text{-}to\text{-}AP}$/$P_{app\ AP\text{-}to\text{-}BL}$ of [^{3}H]-digoxin across Caco-2, MDCK-WT, and MDCK-MDR1 cell monolayers were 14, 8.4, and 33, respectively. These ratios were decreased to 1.1 in the presence of P-gp specific inhibitor GF102918 (2 μM) (25). The ratios of $P_{app\ BL\text{-}to\text{-}AP}$/$P_{app\ AP\text{-}to\text{-}BL}$ of [^{3}H]-vinblastine across Caco-2, MDCK-WT, and MDCK-MRP2 cell monolayers were 18, 15, and 36, respectively. These ratios were decreased to 1.9, 1.7, and 16, respectively, when the P-gp inhibitor GF 120918 (2 μM) was included in the incubation media.

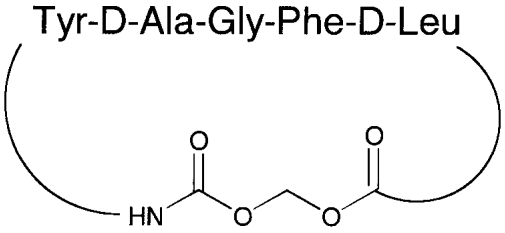

Fig. 1. Chemical structure of AD.

HPLC Analysis

Chromatographic analyses were performed on a Shimadzu LC-10A gradient system (Shimadzu, Inc., Tokyo, Japan) consisting of LC-10 AD pumps, a SCL-10A controller, a SPD-10A UV detector, a SIL-10 A autoinjector equipped with a sample cooler, and two FCV-2A high pressure switching valves. Aliquots of 100 μl from the sample tray were injected into a C-18 reversed-phase column (Vydac #218TP54). Gradient elution was performed at a flow rate of 1 mL/min from 20–50% (v/v) acetonitrile in water using trifluoroacetic acid (0.1%, v/v) as an ion-pairing agent. The eluents were monitored at a wavelength of 214 nm by a UV detector. Data were collected and analyzed using Star Chromatography Workstation and Varian Software (Varian Associates, Inc., Walnut, California). The low limit of quantification (LLQ) of the peptide prodrug was 10 nM. The recovery of the peptide prodrug in the transport experiments was consistently >95%.

Data Analysis

P_{app} values were calculated using the equation:

$$P_{app} = \Delta Q/\Delta t/(A*C_0) \quad (1)$$

Where $\Delta Q/\Delta t$ is the linear appearance rate of mass in the receiver solution, A is the filter/cell surface area (4.71 cm^2), and C_0 is the initial concentration of the test compounds.

The net efflux of a test compound was assessed by calculating the ratio of P_{app} in the BL-to-AP direction vs. P_{app} in the AP-to-BL direction ($P_{app\ BL\text{-}to\text{-}AP}/P_{app\ AP\text{-}to\text{-}BL}$). A ratio of substantially greater than 1.0 indicates a net efflux of the solute.

RESULTS

Expression Levels of P-gps and MRP2s in Caco-2, MDCK-WT, MDCK-MDR1, and MDCK-MRP2 Cells

For MDCK cells transfected with the genes for human P-gp and MRP2 to be useful in elucidating the profile of AD as a substrate for these efflux transporters, functional expression of these proteins needed to be demonstrated. As shown in Figure 1, all three cell lysates (Caco-2, MDCK-WT, and MDCK-MDR1) cross-reacted with P-gp antibody Ab-1 and exhibited two bands on PAGE with the apparent molecular weights of ~150 kDa and ~170 kDa. MDCK-MDR1 cells overexpress the lower molecular weight isoform of P-gp, which migrates with an apparent molecular weight of 150 kDa (Fig. 2, lane C). P-gp antibody C219 was also used in Western blotting experiments. The resultant Western blots were similar to those observed with using antibody Ab-1 (data not shown). These results are consistent with our earlier observations that suggest the possibility that MDR1 transfected in MDCK cells is less extensively glycosylated than canine P-gp in MDCK cells or MDR1 in Caco-2 cells (23). With respect to MRP2, all three cell lysates cross-reacted with MRP2 antibody and exhibited two bands on PAGE with the apparent molecular weights of ~150 kDa and ~190 kDa (Fig. 3). MDCK-MRP2 cells express high levels of MRP2 isoform with an apparent molecular weight of 150 kD, again consistent with the earlier results (Fig. 3, lane C) (24). These results

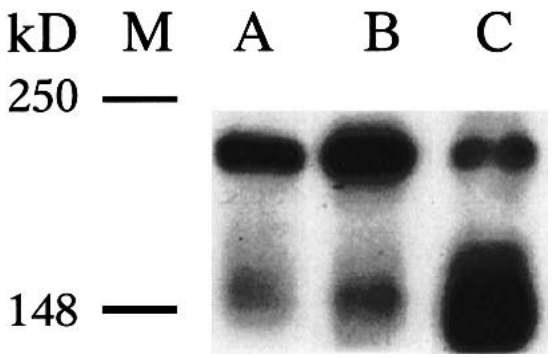

Fig. 2. Western blotting of P-gps in the total cell lysates from Caco-2, MDCK-WT, and MDCK-MDR1 cell monolayers. Proteins (10 μg) were size-fractionated in 6% Tris-glycine polyacrylamide gel in 0.1% SDS Tris-glycine buffer. After electroblotting, P-gps were stained with mdr Ab-1 and the protein-antibody interaction was visualized using the chemiluminescence technique as described in Materials and Methods. Lane A: Caco-2 cell line; B: MDCK-WT cell line; C: MDCK-MDR1 cell line. M: Molecular weight marker.

suggested the possibility that human MRP2 transfected into MDCK cells is less extensively glycosylated than canine MRP2 in MDCK cells or human MRP2 in Caco-2 cells (24). When the functional expression of P-gps and MRP2s was determined in these cell lines using [^{3}H]-digoxin and [^{3}H]-vinblastine, respectively, the MDCK cells transfected with the genes for human P-gp and MRP2 showed the higher efflux activity (data not shown), which is consistent with our earlier data (23,24).

Transport of AD across Caco-2 Cell Monolayers

Table I shows the P_{app} values of AD across Caco-2 cell monolayers in the absence and presence of GF120918 and/or CsA. GF120918 is a known inhibitor of P-gp (25) and was shown in previous studies in our laboratory (23) to completely inhibit the efflux of [^{3}H]-digoxin in this cell line at the concentration used in these studies. To evaluate whether MRP2 contributed to the polarized efflux of AD in these cell lines, CsA, a known inhibitor for P-gp and MRP2 (26,27), was also used in these experiments. CsA was shown in previous studies

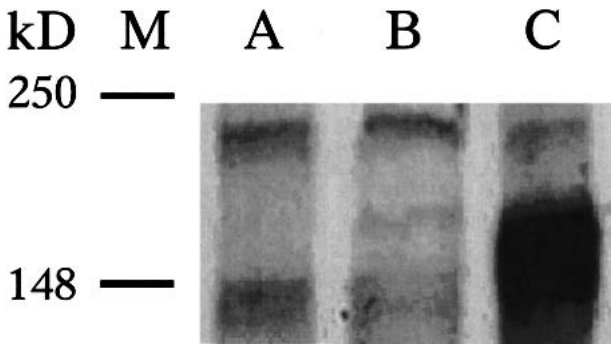

Fig. 3. Western blotting of MRP2 in the total cell lysates from Caco-2, MDCK-WT, and MDCK-MRP2 cell monolayers. Proteins (20 μg) were size-fractionated in 6% Tris-glycine polyacrylamide gel in 0.1% SDS Tris-glycine buffer. After electroblotting, MRP2 was stained with M_2I-4 and the protein-antibody interaction was visualized using the chemiluminescence technique as described in Materials and Methods. Lane A: Caco-2 cell line; B: MDCK-WT cell line; C: MDCK-MRP2 cell line. M: Molecular weight marker.

Table I. P_{app} Values of AD across Caco-2 Cell Monolayers in the Presence and Absence of Known Inhibitors of P-gp and MRP2

Treatment	P_{app}*10^7 (cm/s)		Ratio ($P_{app\ BL\text{-}to\text{-}AP}$/ $P_{app\ AP\text{-}to\text{-}BL}$)
	AP-to-BL	BL-to-AP	
—	0.46 ± 0.08	45.59 ± 3.45	99
GF120918 (2 μM)	1.19 ± 0.09	13.03 ± 0.75	11
CsA (25 μM)	1.59 ± 0.32	17.71 ± 1.21	11
GF120918 (2 μM)+CsA (25 μM)	1.96 ± 0.16	6.01 ± 0.33	3.0

Note: P_{app} values of AD were measured in the absence or the presence of GF120918 (2 μM), CsA (25 μM), or GF120918 (2 μM) and CsA (25 μM) in Caco-2 cells as described in Materials and Methods. P_{app} values are presented as mean ± SD (n = 3).

Table II. P_{app} Values of AD across MDCK-WT Cell Monolayers in the Presence and Absence of Known Inhibitors of P-gp and MRP2

Treatment	P_{app}*10^7 (cm/s)		Ratio ($P_{app\ BL\text{-}to\text{-}AP}$/ $P_{app\ AP\text{-}to\text{-}BL}$)
	AP-to-BL	BL-to-AP	
—	1.13 ± 0.41	5.32 ± 0.33	4.7
GF120918 (2 μM)	1.28 ± 0.26	4.12 ± 0.31	3.2
CsA (25 μM)	1.24 ± 0.20	2.72 ± 0.24	2.2
GF120918 (2 μM)+CsA (25 μM)	2.06 ± 0.17	2.52 ± 0.13	1.2

Note: P_{app} values of AD were measured in the absence or the presence of GF120918 (2 μM), CsA (25 μM), or GF120918 (2 μM) and CsA (25 μM) in MDCK-WT cells as described in Materials and Methods. P_{app} values are presented as mean ± SD (n = 3).

(24) to completely inhibit the efflux of [^{3}H]- vinblastine in this cell line at the concentration used in the present studies. As shown in Figure 4 and Table I, AD exhibited high polarized efflux in Caco-2 cells (i.e., $P_{app\ BL\text{-}to\text{-}AP} >> P_{app\ AP\text{-}to\text{-}BL}$). The ratio of $P_{app\ BL\text{-}to\text{-}AP}/P_{app\ AP\text{-}to\text{-}BL}$, which is used here as an indicator of efflux activity, was 99 (Table I). In the presence of GF120918 (2 μM), $P_{app\ AP\text{-}to\text{-}BL}$ increased and $P_{app\ BL\text{-}to\text{-}AP}$ decreased, resulting a $P_{app\ BL\text{-}to\text{-}AP}/P_{app\ AP\text{-}to\text{-}BL}$ ratio equal to 11 (Table I). The inhibitory effect of CsA (25 μM) on the polarized efflux of AD in Caco-2 cells was similar to that observed with GF120918 (2 μM), resulting in a $P_{app\ BL\text{-}to\text{-}AP}/P_{app\ AP\text{-}to\text{-}BL}$ ratio of 11. A cocktail of GF120918 (2 μM) and CsA (25 μM) further decreased the $P_{app\ BL\text{-}to\text{-}AP}/P_{app\ AP\text{-}to\text{-}BL}$ ratio to 3.0 (Fig. 4, Table I).

Transport of AD across MDCK-WT Cell Monolayers

MDCK-WT cells also showed polarized efflux of AD with a $P_{app\ BL\text{-}to\text{-}AP}/P_{app\ AP\text{-}to\text{-}BL}$ ratio of 4.7 (Table II). The polarized efflux of AD was significantly less in MDCK-WT cells than in Caco-2 cells as measured by the $P_{app\ BL\text{-}to\text{-}AP}/P_{app\ AP\text{-}to\text{-}BL}$ ratios (i.e., 4.7 vs. 99). GF120918 (2 μM) and CsA (25 μM) decreased $P_{app\ BL\text{-}to\text{-}AP}$ values, resulting in decreased $P_{app\ BL\text{-}to\text{-}AP}/P_{app\ AP\text{-}to\text{-}BL}$ ratios of 3.2 and 2.2, respectively. The cocktail of GF120918 (2 μM) and CsA (25 μM) almost completely inhibited the efflux of AD in MDCK-WT cells, producing a $P_{app\ BL\text{-}to\text{-}AP}/P_{app\ AP\text{-}to\text{-}BL}$ ratio of 1.2.

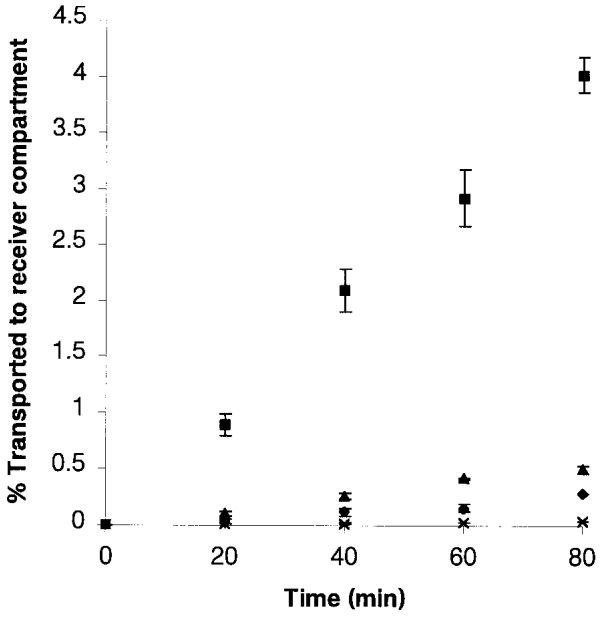

Fig. 4. Bidirectional transport of AD across Caco-2 cell monolayers in the absence and presence of inhibitors. ♦: BL-to-AP no inhibitor; ×: BL-to-AP + GF120918 (2 μM) + CsA (25 μM); ♦: AP-to-BL + GF120918 (2 μM) + CsA (25 μM); ×: AP-to-BL no inhibitor. Data are presented as mean ± SD (n = 3).

Transport of AD across MDCK-MDR1 Cell Monolayers

As shown in Table III, the polarized efflux of AD was higher in MDCK-MDR1 cell monolayers than in MDCK-WT cell monolayers (i.e., the $P_{app\ BL\text{-}to\text{-}AP}/P_{app\ AP\text{-}to\text{-}BL}$ ratios were10 vs. 4.7, respectively). This polarized efflux of AD in MDCK-MDR1 could be significantly inhibited by inclusion of CsA (25 μM) or GF120918 (2 μM) in the incubation mixture (Table 3). In the presence of the mixture of GF120918 (2 μM) and CsA (25 μM), $P_{app\ AP\text{-}to\text{-}BL}$ increased and $P_{app\ BL\text{-}to\text{-}AP}$ decreased, resulting a $P_{app\ BL\text{-}to\text{-}AP}/P_{app\ AP\text{-}to\text{-}BL}$ ratio equal to 1.8.

Transport of AD across MDCK-MRP2 Cell Monolayers

MDCK-MRP2 cells exhibited less polarized efflux of AD than MDCK-MDR1 cells (i.e., 5.8 vs. 10, respectively, Tables III and IV), as measured by the $P_{app\ BL\text{-}to\text{-}AP}/P_{app\ AP\text{-}to\text{-}BL}$ ratios. MDC-MRP2 cells exhibited approximately the same polarized efflux of AD as MDCK-WT cells (i.e., the ratios

Table III. P_{app} Values of AD across MDCK-MDR1 Cell Monolayers in the Presence and Absence of Known Inhibitors of P-gp and MRP2

Treatment	P_{app}*10^7 (cm/s)		Ratio ($P_{app\ BL\text{-}to\text{-}AP}$/ $P_{app\ AP\text{-}to\text{-}BL}$)
	AP-to-BL	BL-to-AP	
—	0.74 ± 0.37	7.18 ± 0.29	10
GF120918 (2 μM)	1.15 ± 0.09	4.01 ± 0.22	3.5
CsA (25 μM)	1.61 ± 0.26	4.21 ± 0.35	2.6
GF120918 (2 μM)+CsA (25 μM)	1.78 ± 0.18	3.11 ± 1.8	1.8

Note: P_{app} values of AD were measured in the absence or the presence of GF120918 (2 μM). CsA (25 μM), or GF120918 (2 μM) and CsA (25 μM) in MDCK-MDR1 cells as described in Materials and Methods. P_{app} values are presented as mean ± SD (n = 3).

Table IV. P_{app} Values of AD across MDCK-MRP2 Cell Monolayers in the Presence and Absence of Known Inhbitors of P-gp and MRP2

Treatment	P_{app}*10^7 (cm/s)		Ratio ($P_{app\ BL\text{-}to\text{-}AP}$/ $P_{app\ AP\text{-}to\text{-}BL}$)
	AP-to-BL	BL-to-AP	
—	1.43 ± 0.13	8.30 ± 0.69	5.8
GF120918 (2 μM)	1.69 ± 0.21	6.24 ± 0.21	3.6
CsA (25 μM)	1.37 ± 0.18	4.83 ± 0.77	3.5
GF120918 (2 μM)+CsA (25 μM)	1.95 ± 0.13	4.50 ± 0.21	2.3

Note: P_{app} values of AD were measured in the absence or the presence of GF120918 (2 μM), CsA (25 μM), or GF120918 (2 μM) and CsA (25 μM) in MDCK-MRP2 cells as described in Materials and Methods. P_{app} values are presented as mean ± SD (n = 3).

were 5.8 vs. 4.7, respectively, Tables II and IV). In the presence of GF120918 (2 μM) or CsA (25 μM), $P_{app\ BL\text{-}to\text{-}AP}$ decreased slightly, resulting in $P_{app\ BL\text{-}to\text{-}AP}/P_{app\ AP\text{-}to\text{-}BL}$ ratios of 3.6 and 3.5, respectively. The mixture of GF120918 (2 μM) and CsA (25 μM) increased $P_{app\ AP\text{-}to\text{-}BL}$ and decreased $P_{app\ BL\text{-}to\text{-}AP}$, resulting in a $P_{app\ BL\text{-}to\text{-}AP}/P_{app\ AP\text{-}to\text{-}BL}$ ratio of 2.3.

DISCUSSION

P-gp was first found in cancer cells in 1976 and correlated with the drug resistance phenomenon (28). In humans, P-gp has also been shown to be widely expressed in the normal tissues such as gastrointestinal mucosa, liver, pancreas, brain, and kidney (29). In the human intestine, P-gp is localized on the AP side of intestinal epithelial cells (20). This polarized expression of P-gp suggests that it functions as a secretory detoxifying system; thus, it represents a major barrier impeding drug permeation across the intestinal mucosa (9).

Since the middle 1990s, MRPs have also been shown to restrict drug absorption through the intestinal mucosa and BBB (21). There are at least 7 members in the MRP family. Among MRP transporters, MRP2 is localized on the canalicular membrane of hepatocytes and on the AP side of intestinal mucosal and kidney cells (30). Although MRP2 was originally described as the canalicular multispecific organic anion transporter (cMOAT) (31), it was also found to be functional in multidrug resistance and limiting drug absorption through the intestinal mucosa (32).

In recent years, using Caco-2 cells as a model of the intestinal mucosa has become popular among pharmaceutical scientists (16). In addition to its use in determining the passive diffusion characteristics of drugs/drug candidates (16), this cell culture model has also been used to determine the substrate activity for efflux transporters (20). However, several potential problems exist in using Caco-2 cells to study efflux transporters. One of these relates to the heterogeneous nature of this cell line and the resulting variability from laboratory to laboratory in the expression of efflux transporters (Benet, L. Z., UCSF, personal communication). Another problem is that even if one has Caco-2 cells that exhibit polarized efflux, the specific efflux transporter (e.g., P-gp vs. MRP2) involved in restricting a solute's permeation across a Caco-2 cell monolayer is difficult to elucidate. Therefore, efforts have been made to establish cell lines transfected with a human gene (e.g., MDCK-MDR1cells, MDCK-MRP2 cells) that lead to a high expression of a gene product (21). These transfected cell lines overexpress one transporter [e.g., human P-gp (MDR1) or MRP2] and make a "purer" system for investigation of structure–transport relationships. In these studies, we have attempted to use these transfected MDCK cells to elucidate the structure–transport relationships for AD.

It is worth noting that the expression levels of P-gp in the Caco-2 cells used in our laboratory are higher than the expression levels of MRP2 (Fig. 2, lane A vs. Fig. 3, lane A). Evidence in support of this conclusion includes our observation that the polarized efflux of [^{3}H]-vinblastine [a substrate for P-gp and MRP2 (32)] in this Caco-2 cell line is partially inhibited by GF120918 (2 μM), a known specific P-gp inhibitor (25), but completely inhibited by a CsA (25 μM), a known inhibitor for P-gp and MRP2 (26,27). These data suggest that the polarized efflux of [^{3}H]-vinblastine in Caco-2 cells is mediated by P-gp as well as MRP2 (24).

The bi-directional transport data for AD generated in Caco-2 cells indicate that it is a good substrate of one or more of the efflux systems present in Caco-2 cells (Table I). GF120918 (2 μM) significantly inhibited this polarized efflux, i.e., the $P_{app\ BL\text{-}to\text{-}AP}/P_{app\ AP\text{-}to\text{-}BL}$ ratio decreased from 99 to 11. GF120918 is a specific inhibitor for P-gp at low concentrations (<~1 μM). It has also been reported to inhibit breast cancer resistance protein (MXR) at the higher concentrations (10 μM) (33,34). These data indicate that the polarized efflux of AD in Caco-2 cells is probably due mainly to the presence of P-gp. Further confirmation of this hypothesis was obtained by doing inhibition studies with CsA, which is an inhibitor for both P-gp and MRP2 (27). The inhibitory effects of CsA on the efflux of AD in Caco-2 cells was similar to that observed with GF120918. The similarity in the effects of GF120918 and CsA on AD efflux in Caco-2 cells can be interpreted in two possible ways. One interpretation is that AD is a good substrate for P-gp and a poor substrate for MRP2. Based on the results described in this manuscript using MDCK-MDR1 and MDCK-MRP2 cells, we feel that this is the most reasonable interpretation of the data. The second possible interpretation is that the MRP2 expression levels in our Caco-2 cells are so low that their MRP2 has no functional significance. This second possibility seems unlikely because earlier our laboratory (24) showed that vinblastine, a known substrate for P-gp and MRP2 (32), is effluxed and this efflux is completely inhibited by CsA (24). It is interesting to note that the cocktail of GF120918 and CsA could not totally inhibit the polarized efflux of AD (i.e., the $P_{app\ BL\text{-}to\text{-}AP}/P_{app\ AP\text{-}to\text{-}BL}$ ratio was 3). This effect is different from what our laboratory observed with digoxin, a known substrate for P-gp (24), and vinblastine, a known substrate of MRP2 (32). One possibility is that AD is a substrate for a yet unknown efflux transporter in Caco-2 cells.

Based on our earlier data with MDCK-WT cells (24), it was not surprising that MDCK-WT showed polarized efflux of AD. However, this polarized efflux was significantly less than that observed in Caco-2 cells (Tables I and II). These results were consistent with our data that MDCK-WT cells not only express significant levels of P-gp as measured by Western blotting (Fig. 2) but also exhibit functional polarized efflux of P-gp substrates (e.g., digoxin) (23). MDCK cells are a dog-renal epithelia cell line. When grown onto Transwells®, MDCK cells differentiate into columnar epithelium and form

tight junctions in a shorter period of time than Caco-2 cells (3 days vs. 21days) (35). MDCK cells and Caco-2 cells have been reported to share many common epithelial cell characteristics (36). A good correlation between the permeation results of passively absorbed drugs in Caco-2 cells and MDCK cells (36) suggests that the MDCK cell model may be useful for screening membrane permeability. This suggestion is probably reasonable if one assumes that the drugs are not substrates for P-gp. Therefore, when MDCK-WT cells are used as the model for a permeability screening (36), one should consider this factor when the tested drugs/drug candidates are potential P-gp substrates.

MDCK-MDR1 cells overexpress human P-gp (Fig. 2) and exhibit greater polarized efflux of P-gp substrates than MDCK-WT cells (37). The greater polarized efflux of AD in MDCK-MDR1 cells than in MDCK-WT cells further confirms that AD is a very good substrate for P-gp (Tables II and III). MDCK-MRP2 cells overexpress MRP2 (Fig. 3) and exhibit greater polarized efflux of MRP2 substrates than MDCK-WT cells (32). The polarized efflux of AD was marginally greater in MDCK-MRP2 cells as compared to MDCK-WT cells (Tables II and IV). Furthermore, GF120918 (P-gp inhibitor) and CsA (P-gp and MRP2 inhibitor) had similar inhibition effects on this polarized efflux. These results suggest that AD is a very poor substrate for MRP2, and the polarized efflux of AD in MDCK-MRP2 cells might result mainly from the functional efflux activities of native P-gp in these cells.

P-gp is highly expressed on the apical surface of intestinal epithelia cells, the biliary surface of hepatocytes, and capillary endothelial cells of brain (19). Based on this tissue distribution, it has been proposed that P-gp functions as a secretory detoxifying system; thus, it represents a major barrier impeding drugs permeation across the intestinal mucosa (9) and BBB (19). The good P-gp substrate activity of AD, therefore, suggests that this prodrug will have low intestinal permeability and low BBB penetration. Indeed, the *in vivo* results generated in our laboratory using *in situ* perfused rat ileum model and *in situ* perfused rat brain model are consistent with this prediction, i.e., AD exhibited brain and intestinal permeation similar to that of DADLE, even though it has more favorable physicochemical properties. This low permeability of AD could be increased several fold by inclusion of a P-gp inhibitor (e.g., GF120918) in the perfusates (Chen et al, unpublished data).

In summary, these data suggest that AD is a much better substrate for P-gp than MRP2, and that the restricted permeation of this cyclic prodrug in Caco-2 cells, in the intestinal mucosa, and in BBB is probably due primarily to its substrate activity for P-gp.

ACKNOWLEDGMENTS

The authors thank Drs. Raymond Evers and Piet Borst (The Netherlands Cancer Institute, Amsterdam, The Netherlands) for providing the MDCK-MDR1 and MDCK-MRP2 cell lines, and Dr. Kenneth Brouwer (GlaxoSmithKline, Research Triangle Park, North Carolina) for the sample of GF120918. The work was supported by a grant from the United States Public Health Service (DA09315).

REFERENCES

1. U. Bickel, T. Yoshikawa, and W. M. Pardridge. Delivery of peptides and proteins through the blood-brain barrier. *Adv. Drug Deliv. Rev.* **46**:247–279 (2001).
2. C. L. Neilan, T. M. Nguyen, P. W. Schiller, and G. W. Pasternak. Pharmacological characterization of the dermorphin analog. *Eur. J. Pharmacol.* **419**:15–23 (2001).
3. U. B. Kompella and V. H. Lee. Delivery systems for penetration enhancement of peptide and protein drugs: design considerations. *Adv. Drug Deliv. Rev.* **46**:211–245 (2001).
4. T. K. Sawyer. (1995) *Peptidomimetic Design and Chemistry Approaches to Peptide Metabolism*, American Chemical Society, Washington, DC.
5. R. T. Borchardt, J. Aube, T. J. Siahaan, S. Gangwar, and G. M. Pauletti. Improvement of oral peptide bioavailability: Peptidomimetics and prodrug strategies. *Adv. Drug Deliv. Rev.* **27**:235–256 (1997).
6. L. Prokai. Peptide drug delivery into the central nervous system. *Prog. Drug Res.* **51**:95–131 (1998).
7. V. J. Wacher, J. A. Silverman, Y. Zhang, and L. Z. Benet. Role of P-glycoprotein and cytochrome P450 3A in limiting oral absorption of peptides and peptidomimetics. *J. Pharm. Sci.* **87**:1322–1330 (1998).
8. J. W. Polli, J. L. Jarrett, S. D. Studenberg, J. E. Humphreys, S. W. Dennis, K. R. Brouwer, and J. L. Woolley. Role of P-glycoprotein on the CNS disposition of amprenavir (141W94), an HIV protease inhibitor. *Pharm. Res.* **16**:1206–1212 (1999).
9. V. J. Wacher, L. Salphati, and L. Z. Benet. Active secretion and enterocytic drug metabolism barriers to drug absorption. *Adv. Drug Deliv. Rev.* **46**:89–102 (2001).
10. G. M. Pauletti, S. Gangwar, B. Wang, and R. T. Borchardt. Esterase-sensitive cyclic prodrugs of peptides: evaluation of a phenylpropionic acid promoiety in a model hexapeptide. *Pharm. Res.* **14**:11–17 (1997).
11. G. M. Pauletti, S. Gangwar, F. W. Okumu, T. J. Siahaan, V. J. Stella, and R. T. Borchardt. Esterase-sensitive cyclic prodrugs of peptides: evaluation of an acyloxyalkoxy promoiety in a model hexapeptide. *Pharm. Res.* **13**:1615–1623 (1996).
12. O. S. Gudmundsson, G. M. Pauletti, W. Wang, D. Shan, H. Zhang, B. Wang, and R. T. Borchardt. Coumarinic acid-based cyclic prodrugs of opioid peptides that exhibit metabolic stability to peptidases and excellent cellular permeability. *Pharm. Res.* **16**:7–15 (1999).
13. S. Gangwar, S. D. Jois, T. J. Siahaan, D. G. Vander Velde, V. J. Stella, and R. T. Borchardt. The effect of conformation on membrane permeability of an acyloxyalkoxy-linked cyclic prodrug of a model hexapeptide. *Pharm Res.* **13**:1657–1662 (1996).
14. A. Bak, T. J. Siahaan, O. S. Gudmundsson, S. Gangwar, G. J. Friis, and R. T. Borchardt. Synthesis and evaluation of the physicochemical properties of esterase-sensitive cyclic prodrugs of opioid peptides using an (acyloxy)alkoxy linker. *J. Pept. Res.* **53**:393–402 (1999).
15. A. Bak, O. S. Gudmundsson, G. J. Friis, T. J. Siahaan, and R. T. Borchardt. Acyloxyalkoxy-based cyclic prodrugs of opioid peptides: evaluation of the chemical and enzymatic stability as well as their transport properties across Caco-2 cell monolayers. *Pharm. Res.* **16**:24–29 (1999).
16. P. Artursson, K. Palm, and K. Luthman. Caco-2 monolayers in experimental and theoretical predictions of drug transport. *Adv. Drug Deliv. Rev.* **46**:27–43 (2001).
17. R. T. Borchardt. The application of cell culture systems in drug discovery and development. *J. Drug Target.* **3**:179–182 (1995).
18. C. Bailey, P. Bryla, and A. Malick. The use of the intestinal epithelial cell culture model, Caco-2, in pharmaceutical development. *Adv. Drug Deliv. Rev.* **22**:85–103 (1996).
19. A. H. Schinkel, J. J. Smit, O. van Tellingen, J. H. Beijnen, E. Wagenaar, L. van Deemter, C. A. Mol, M. A. van der Valk, E. C. Robanus-Maandag, H. P. te Riele, A. J. M. Berns, and P. Borst. Disruption of the mouse mdr1a P-glycoprotein gene leads to a deficiency in the blood-brain barrier and to increased sensitivity to drugs. *Cell* **77**:491–502 (1994).
20. J. Hunter, M. A. Jepson, T. Tsuruo, N. L. Simmons, and B. H. Hirst. Functional expression of P-glycoprotein in apical membranes of human intestinal Caco-2 cells. Kinetics of vinblastine

secretion and interaction with modulators. *J. Biol. Chem.* **268**: 14991–14997 (1993).
21. P. Borst, R. Evers, M. Kool, and J. Wijnholds. The multidrug resistance protein family. *Biochim. Biophys. Acta.* **1461**:347–357 (1999).
22. J. Gao, E. D. Hugger, M. S. Beck-Westermeyer, and R. T. Borchardt. In H. Doyle, J. B. Griffiths, and D. J. Newell (eds.), *Current Protocols in Pharmacology, Vol. 7.2*, John Wiley & Sons, Inc., New York, 2000 pp. 1-23.
23. F. Tang, H. Kazutoshi, and R. T. Borchardt. Are MDCK cells transfected with the human MDR1 gene a good model of the human intestinal mucosa? *Pharm. Res*. **19**:765–772 (2002).
24. F. Tang, H. Kazutoshi, and R. T. Borchardt. Are MDCK cells transfected with the human MRP2 gene a good model of the human intestinal mucosa? *Pharm. Res*. **19**:773–779 (2002).
25. S. P. Letrent, G. M. Pollack, K. R. Brouwer, and K. L. Brouwer. Effects of a potent and specific P-glycoprotein inhibitor on the blood-brain barrier distribution and antinociceptive effect of morphine in the rat. *Drug Metab Dispos.* **27**:827–834 (1999).
26. A. J. Smith, U. Mayer, A. H. Schinkel, and P. Borst. Availability of PSC833, a substrate and inhibitor of P-glycoproteins, in various concentrations of serum. *J. Natl. Cancer Inst.* **90**:1161–1166 (1998).
27. A. T. Nies, T. Cantz, M. Brom, I. Leier, and D. Keppler. Expression of the apical conjugate export pump, Mrp2, in the polarized hepatoma cell line, WIF-B. *Hepatology* **28**:1332–1340 (1998).
28. R. L. Juliano and V. Ling. A surface glycoprotein modulating drug permeability in Chinese hamster ovary cell mutants. *Biochim. Biophys. Acta.* **455**:152–162 (1976).
29. A. H. Schinkel, C. A. Mol, E. Wagenaar, L. van Deemter, J. J. Smit, and P. Borst. Multidrug resistance and the role of P-glycoprotein knockout mice. *Eur. J .Cancer* **31A**:1295–1298 (1995).
30. J. Konig, A. T. Nies, Y. Cui, I. Leier, and D. Keppler. Conjugate export pumps of the multidrug resistance protein (MRP) family: localization, substrate specificity, and MRP2-mediated drug resistance. *Biochim. Biophys Acta.* **1461**:377–394 (1999).
31. P. L. Jansen, W. H. Peters, and W. H. Lamers. Hereditary chronic conjugated hyperbilirubinemia in mutant rats caused by defective hepatic anion transport. *Hepatology* **5**:573–579 (1985).
32. R. Evers, M. Kool, L. van Deemter, H. Janssen, J. Calafat, L. C. Oomen, C. C. Paulusma, R. P. Oude Elferink, F. Baas, A. H. Schinkel, and P. Borst. Drug export activity of the human canalicular multispecific organic anion transporter in polarized kidney MDCK cells expressing cMOAT (MRP2) cDNA. *J. Clin. Invest.* **101**:1310–1319 (1998).
33. F. Hyafil, C. Vergely, P. Du Vignaud, and T. Grand-Perret. In vitro and in vivo reversal of multidrug resistance by GF120918, an acridonecarboxamide derivative. *Cancer Res.* **53**:4595–4602 (1993).
34. M. de Bruin, K. Miyake, T. Litman, R. Robey, and S. E. Bates. Reversal of resistance by GF120918 in cell lines expressing the ABC half-transporter, MXR. *Cancer Lett.* **146**:117–126 (1999).
35. M. J. Cho, D. P. Thompson, C. T. Cramer, T. J. Vidmar, and J. F. Scieszka. The Madin Darby canine kidney (MDCK) epithelial cell monolayer as a model cellular transport barrier. *Pharm. Res.* **6**:71–77 (1989).
36. J. D. Irvine, L. Takahashi, K. Lockhart, J. Cheong, J. W. Tolan, H. E. Selick, and J. R. Grove. MDCK (Madin-Darby canine kidney) cells: A tool for membrane permeability screening. *J. Pharm. Sci.* **88**:28–33 (1999).
37. R. Evers, N. H. Cnubben, J. Wijnholds, L. van Deemter, P. J. van Bladeren, and P. Borst. Transport of glutathione prostaglandin A conjugates by the multidrug resistance protein 1. *FEBS Lett.* **419**: 112–116 (1997).